IRAQI JOURNAL OF APPLIED PHYSICS
Vol. 22, No. 3, July-September 2026, pp. 504-512

Investigation of Structural Optical Electrical and Dielectric Properties of Solid Blend Electrolytes Based on Chitosan:Polyaniline Incorporating with NaI and LiI

Elaaf A. Swady
Mohammed K. Jawad*

Department of Physics,
College of Science,
University of Baghdad,
Baghdad, IRAQ
* Corresponding author email:
mohamedkadhom66@gmail.com

Solid polymer electrolytes based on biopolymer blends have attracted significant interest for sustainable electrochemical applications. Blend electrolytes were prepared through solvent cast method and under a controlled environment in the laboratory. The electrolyte consisted of a 90:10 Cs:PANI ratio with different concentrations of salt (LiI and/or NaI) and a fixed quantity of iodine (10 wt.%) of the salt. The highest values of the electrical conductivity for electrolytes with LiI were 0.78 $S.cm^{-1}$ while for electrolytes with NaI 0.64 $S.cm^{-1}$ at room temperature. The conductivity elevating with raising salts concentration and with increase temperature range 303-353 K. The structural interactions between the polymer host and ionic species were investigated using FTIR spectroscopy. The FTIR results confirmed coordination between Li^+/Na^+ ions and the polar functional groups of chitosan and polyaniline. UV-visible analysis revealed enhanced optical absorption and a reduction in optical band gap with increasing salt concentration.

Keywords: Blend biopolymer; Electrolyte; Iodide salts; AC conductivity
Received: 26 January 2026; Revised: 25 March 2026; Accepted: 1 April 2026; Published: 1 July 2026

1. Introduction

The conductive polymers have received significant investigations as they are readily produced, highly electrically conductive, stable to the environment, relatively low cost, and have unique redox behavior of electrons. These polymers are a special category of materials that provide the plastics with their process ability and flexibility in addition to the electrical and optical properties of metals and semiconductors. The conducting polymers that are commonly used are made of carbon, hydrogen and other hetero atoms like nitrogen or sulfur and are conjugated by the double bonds along the polymer backbone. Examples of these include polythiophene (PTh), polyaniline (PANI) and polypyrrole (PPy) [1]. Use of non-degradable materials has been found to be one of the greatest challenges in the current food packaging, leading to pollution of the environment. Therefore, recent research efforts have concentrated on the preparation of biodegradable, renewable and biocompatible packaging materials that have the biopolymers as substrates. They have been used in edible films and coatings and have demonstrated the capability to inhibit moisture movement, nasty aromas and oxygen permeation. They are however limited in their mechanical strength and bad thermal stability limiting their broader industrial application [2]. To overcome the plastic packaging constraint, scientists have incorporated two or more polymers into producing film composite so that the composite films can enhance mechanical, thermal and physical characteristics of the films. Moreover, the synergies between natural and synthetic polymers may also be made to increase performance and decrease the cost of production with a view to a large number of applications [3].

Lithium-ion batteries (also referred to as LIBs) are now becoming nearly unavoidable in the portables, electric vehicles (EVs), and energy storage systems used at large-scale. Their use has been extensively spread as they have a high energy density, high operating voltage and a good cycling instability. Conventional LIBs are capable of volumetric energy densities of about 770 Wh/L as well as gravimetric energy densities of circa 300 Wh/kg. Although these have these benefits, their potential is still inadequate to cover the increasing world energy needs. Also, volatile and flammable organic liquid electrolytes are not only very dangerous according to their hazards but also on a large scale, specifically EVs and power grids. An even bright alternative is solid-state electrolytes (SSEs), which are much safer and allow one to apply lithium-metal anodes and do not require polymer separators, which simplifies the manufacturing of a battery structure [4,5].

Recently, the improvement of solid polymer electrolytes (SPEs) has attracted considerable attention because of its possible application as solid ionic conductors in other electrochemical applications such as lithium-ion batteries, super capacitors and fuel cells. Polymer blending is one of the methods that has been adopted among others to enhance the performance of electrolytes as compared with using single polymers. The process allows creating innovative polymeric material of high ionic conductivity and mechanical stability and structural compatibility [6]. The increasing global need of safe, sustainable, and

affordable energy storage systems (ESS) has triggered the increase in the study of the alternative to the traditional lithium-ion battery (LIBs). Although the LIBs are the current reigning powers in the portable electronics and electric vehicles because of their high energy density and long sacrificial cycles, the shortage of lithium elements, and increasing price of cobalt have prompted the identification of alternative electrode chemistries. Sodium-ion batteries (SIBs) have emerged as promising candidates because sodium is the fifth most abundant element on Earth and exhibits electrochemical behavior similar to lithium. Although Na^+ possesses a larger ionic radius (0.99 Å) than Li^+ (0.69 Å) and a slightly higher redox potential, resulting in slower kinetics and larger volume expansion, recent progress in electrode design and material optimization continues to improve SIB performance. Consequently, SIBs represent a viable low-cost and sustainable option for next-generation ESS [7]. Electrochemical energy storage devices have been considered an excellent resource to provide low-cost and biodegradable energy. Initially, many biopolymers such as pectin, cellulose, starch, dextrin, and even more have been studied for their application to solid electrolyte membranes [8]. In this study, Lithium and sodium iodide salts were selected due to their high dissociation ability and compatibility with polymer electrolyte systems. Lithium ions (Li^+) possess a small ionic radius and high charge density, which facilitates strong coordination with polar functional groups such as –OH and –NH present in chitosan and polyaniline. This interaction enhances ionic mobility and improves ionic conductivity. On the other hand, sodium ions (Na^+) offer a cost-effective and abundant alternative to lithium-based systems, making them attractive for large-scale energy storage technologies such as sodium-ion batteries. Building on this concept, the present work aims to systematically investigate the influence of the LiI-to-NaI weight ratio on the structural, optical, and electrical properties of chitosan–polyaniline (Cs–PANI) blend electrolytes. The ultimate objective is to optimize their performance as bio-based polymer electrolytes for smart materials and energy-related applications.

2. Experimental Part

The raw materials include chitosan (medium molecular weight, viscosity 300–1000 cps, ≥98% purity, Glentham Life Sciences, UK), and aniline (≥99.5%, Sigma-Aldrich). The average molecular weight of chitosan was approximately 1250000 Da. Lithium iodide (LiI), sodium iodide (NaI), iodine (I_2) and polyaniline with purity 99% were all purchased from Sigma-Aldrich.

To prepare chitosan/polyaniline (Cs/PANI) blend, initially, 1 g of chitosan (Cs) was gradually dissolved in 60 mL of 1% acetic acid solution under continuous magnetic stirring at 300 rpm for 2 hours at room temperature (25±1 °C). The polymer was added slowly to prevent lump formation, which can occur if Cs is introduced all at once due to its high viscosity and strong intermolecular hydrogen bonding. This was stirred and the result was a clear and homogenous Cs solution. 0.1 g of PANI was dissolved in 5 mL of DMSO with continues stirring and made sure that the solution was thoroughly mixed and dispersed. After the solution of PANI became homogeneous it was transferred into the Cs solution in drops with constant stirring being maintained. The product of the process was mixed continuously at room temperature to obtain a homogenous and stable blend solution, which proves the full miscibility of Cs and PANI stages. Lastly, the dissolved solution blend mixture was poured into sterile Petri dishes in order to dry at room temperature giving rise to smooth and flexible Cs/PANI blend films that could be characterized structurally, optically, and electrically. Table (1) summarizes the composition of the made blend.

Table (1) Preparation details of the Cs/PANI blend sample

Sample	Cs + Acetic Acid	PANI + DMSO
M	1 g + 60 mL	0.1 g + 5 mL

The same procedures were repeated to prepare films with varying LiI and/or NaI wt.% of salt and fixed I_2 ratio of (10 wt.% of the salt) as illustrated in tables (2) and (3). The LiI and/or NaI and iodine were dissolved in 3 ml of DMSO, and the resulting mixture was gradually added to the CS: PANI polymer blend. The mixture was stirred for 2 hrs. Finally, to generate a dry, self-supporting film, the solution mixture was poured into several clean, dry plastic Petri dishes and vaporized gradually at 25°C.

Table (2) Composition of NaI-based electrolytes (N-series)

Assignment	Cs+Acetic Acid	PANI+DMSO	NaI (wt.%)	NaI (mg)	I_2 (mg)
N1	1g+60mL	0.1g+5mL	7.5	83	140
N2	1g+60mL	0.1g+5mL	15	165	279
N3	1g+60mL	0.1g+5mL	22.5	248	418
N4	1g+60mL	0.1g+5mL	30	330	559

Table (3) Composition of LiI-based electrolytes (S-series)

Assignment	Cs+Acetic Acid	PANI+DMSO	LiI (wt.%)	LiI (g)	I_2 (g)
S1	1g+60mL	0.1g+5mL	7.5	0.083	0.0156
S2	1g+60mL	0.1g+5mL	15	0.165	0.0313
S3	1g+60mL	0.1g+5mL	22.5	0.248	0.0469
S4	1g+60mL	0.1g+5mL	30	0.330	0.0626

3. Results and Discussion

The FTIR spectra of the Cs/PANI polymer blends containing two different ratios of NiI and iodine are shown in Fig. (1). Both spectra exhibit the characteristic absorption bands typical of pure Cs and PANI, with noticeable variations that indicate doping-induced interactions between the polymeric matrix and

the dopant species. A broad absorption band observed around 3325 cm^{-1} corresponds to the stretching vibrations of –OH and N–H groups associated with chitosan and PANI. A slight shift from 3325 cm^{-1} in sample N1 to 3352 cm^{-1} in sample N4 suggests a weakening of hydrogen-bonding interactions, implying that the introduction of NiI and iodine alters the local bonding environment by coordinating with the amine ($–NH_2$) and hydroxyl (–OH) functional groups.

FTIR data prove that the addition of NiI and iodine does not alter the polymer backbone on the contrary, it leads to the chemical coordination with the help of nitrogen and oxygen groups. The registered changes, especially in the N-H and C-O areas are a good indicator of protonation and coordination of the metal and ligand, thus resulting in alteration of hydrogen bonds and the electron structure. These changes are consistent with the oxidative doping of PANI by iodine and the coordination of Ni^{2+} ions to amine sites, both of which are known to enhance electrical conductivity and improve the structural ordering of conducting polymer blends. Hence, the spectral variations observed between N1 and N4 indicate that a higher dopant concentration in N4 enhances intermolecular interactions, promoting improved charge delocalization and potentially superior electrical and functional performance of the Cs/PANI–NiI composite. The detailed FTIR band assignments for both samples are summarized in table (4) [9,10].

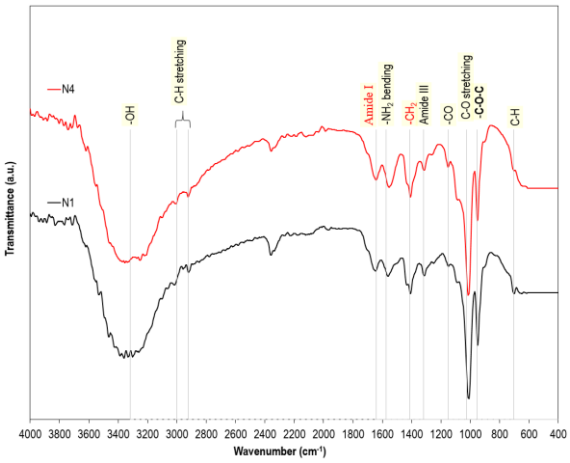

Fig. (1) FTIR spectra of the Cs/PANI blend electrolytes of samples N1, and N4

The FTIR spectra of the Cs/PANI blends introducing with two different LiI salt ratios (S1 and S4) is shown in Fig. (2). The spectra display the characteristic vibrations of the polymer backbone, with modest variations in the hydrogen-bonding environment and in the local bonding of oxygen- and nitrogen-containing functional groups. The broad O–H/N–H stretching band shifts to higher wavenumbers from 3311 cm^{-1} in S1 to 3333 cm^{-1} in S4, indicating a weakening of hydrogen bonding, the bands position was tabulated in table (5). This behavior is consistent with the coordination of Li^+ ions to oxygen and nitrogen atoms, which partially disrupts the original hydrogen bonds in chitosan. The Amide I band remains unchanged at 1649.6 cm^{-1} in both samples, confirming that the main carbonyl/imine environment is preserved. I Instead, Amide III band at 1317.8 changes slightly to 1314.7 cm^{-1} indicating slight alterations in the conformations of the polymer chains due to the insertion of the LiI. The C-O and C-O-C stretching domains are almost the same in the finger print of the two samples and it indicates that glycosidic bondage and the basic saccharidic construct of the chitosan are yet undamaged. The desired differences in the observed spectra between S1 and S4 suggest that LiI acts mostly by disrupting the hydrogen-binding network and makes weak coordination bonds with oxygen and nitrogen locations and not cause the PANI to become highly protonated or oxidized. Amide I and C-O bands remain stable as this indicates that the polymer backbone is also structurally intact. It is anticipated that these minor changes will affect macroscopic characteristics like hydrophilicity, chain packing and ionic/electronic transport, albeit less significantly than the effect by stronger oxidizing dopants [11,12].

Table (4) FTIR band assignments for Cs/PANI blend electrolytes of (N1 and N4)

Band Type	N1	N4
-OH stretch	3325.34	3352.32
C-H stretching	3014.99	3004.20
	2920.54	2923.24
Amide I	1646.78	1644.08
-NH2 bending	1557.72	1552.32
$-CH_2$	1409.30	1406.60
Amide III	1314.84	1314.84
-CO	1152.92	1152.92
C-O stretching	1009.90	1012.59
-C-O-C	945.13	953.22
C-H	702.25	702.25

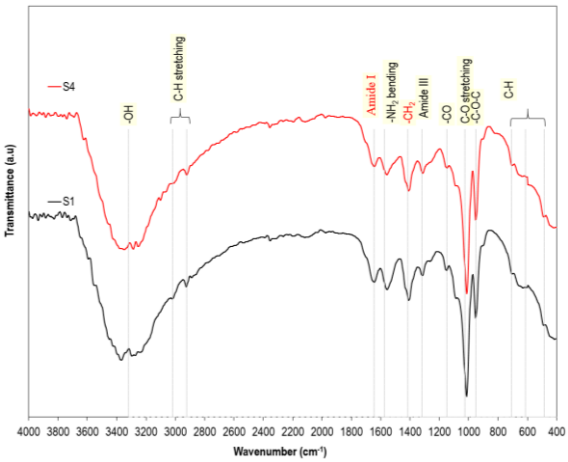

Fig. (2) FTIR spectra of the Cs/PANI blend electrolytes of samples S1 and S4

Table (5) Band positions of Cs/PANI samples with LiI (S1 and S4)

Band Type	S1	S4
-OH stretch	3311.63	3333.33
C-H stretching	3017.05	-
	2924.03	2920.93
Amide I	1649.61	1649.61
-NH2 bending	1559.69	1562.79
-CH2	1410.85	1407.75
Amide III	1317.83	1314.73
-CO	1153.49	1153.49
C-O stretching	1013.95	1013.95
-C-O-C	951.94	951.94
C-H	719.38	713.18
	638.76	598.45
	493.02	493.02

The UV-visible absorption spectra of four samples (N1-N4) are presented in Fig. (3). The spectra indicate that the intensity of absorption is definite with rise in NaI concentration, it clear indication of the increase in intensity of the absorption with an increase in salt content. This increase in optical absorption is due to the fact that there was an increase in charge carrier density and increase in π-conjugation inside the polymer matrix which occurred due to the influence of NaI. The iodide ions (I^-) induces the development of polarons and bipolarons in PANI, which reacts to electronic delocalization along the polymer chain. Consequently, there is an increase in the intensity of electronic transitions, and the absorbance intensity increases tremendously.

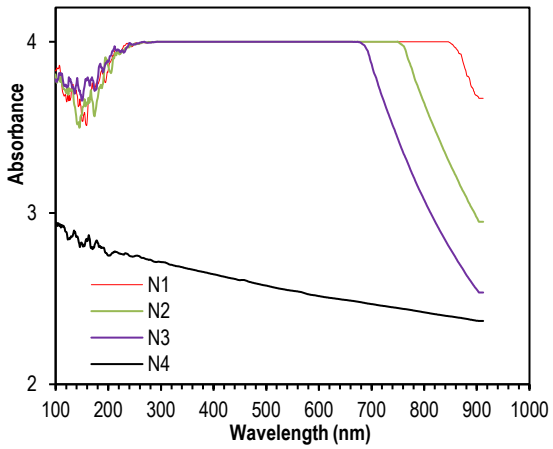

Fig. (3) UV-Visible absorption spectrum of Cs/PANI mixtures (N-series) of different NaI content

The trend in observation indicates that NaI is been effective to improve the electronic connections and optical conductivity of Cs/PANI that has been doped to achieve success in enhancing the optical activity using polymer system [10]. Such an increase in optical absorption may be explained by the fact that existent charge carrier density and conjugation in the polymer matrix increases under the influence of NaI. The iodide ions serve as dopants which promote the formation of polaron and bipolaron in the PANI, which leads to the increase of electronic delocalization of the polymer backbone. This leads to an increased absorption band, and a high absorbance. This tendency shows that the incorporation of NaI is efficient to increase the value of the electronic interaction and conductivity of the Cs–PANI mix, which proves the effective doping and bumped optical activity [13].

Figure (4) shows the UV-visible absorption spectra of Cs/PANI electrolytes with LiI iodide (sample S1 to S4) varying in the concentration of the lithium iodide (LiI). The outcomes indicate a progressive growth of the absorbance as LiI concentration rises and this denotes an apparent alteration of the electronic construction of the blend electrolyte. This strengthened absorbance can be explained by the fact that the concentration of the charge carriers in the polymer is better because of Li^+ ions interaction with the polymer molecular chains (PANI). The small Li^+ ions enter the gaps between the chains of the polymer in which they add intermolecular bonding and density further electron delocalization in the π–π* conjugated system. This occurs as the optical band gap reduces (E_g) because of the narrowing of the energy gap between the valence and conduction bands, thereby making it easier to transport electrons. Therefore, with the incorporation of LiI, there is increased optical absorption and electrical conductivity of the Cs/PANI composite. Sample S1, which has the least LiI content, has the least absorbance and the broadest band gap indicating the poor conductivity of the sample. On the other hand, sample S4, which contains the highest LiI concentration, has the greatest absorbance and the least band gap and this means that the conductivity is greater and charge movement is enhanced. Comprehensively, addition of LiI concentration in the Cs/PANI blend enhances the π–π^* electronic transitions and narrowing optical gap affirming Li^{7+} ions as essential in enhancing the charge transport and electronic performances in the polymer network [14]. In Fig. (5a), the E_g design implies that a threshold is necessary for an electron transition from the valence band to a smaller conduction band; enabling access to the material at lower energies (photons) — a spectral shift towards the red end. Na^+ and I^- ions may cause local structural disruption of the chitosan polymer or react chemically with functional groups additional energy levels within the gap or altering the density of states at the boundaries. Salt increases defects and disorder and lengthens Urbach tails, resulting in absorption at lower energies and a smaller E_g reading. At very low salt concentrations, the effect may be marginal; with increasing concentration, the effect of intermediate states becomes more pronounced and E_g gradually decreases (as shown in N1→N4). The interaction of carriers with each other is improved due to their high concentration in these bands. It can observe from Fig. (5b), the optical spectrum analysis of samples S1–S4 using Tauc's plots

to extract the optical energy gap (E_g) assuming a direct transition. The differences in E_g between the samples are mainly attributed to doping effects and microstructural interference resulting from the difference in the salt ratio (lithium iodide/iodine ions). Increasing the salt concentration leads to the formation of interstitial states within the gap and an increase in charge carrier density in the conductive polymer, thus reducing the optical gap observed in some samples (as in S4). Conversely, a more uniform structure or a different salt concentration may maintain a larger gap. To determine the band gap in addition to the traditional Tauc's relationship as shown in the table (6) below, an alternative method can be used to estimate the optical band gap of polymeric and hybrid materials: the absorption edge method, where the absorption edge is obtained directly from the wavelength at which the absorption increases sharply [15]. The energy band gap (E_g) is calculated using the following equation:

$$\alpha h\nu = A(h\nu - E_g)^2 \quad (1)$$

where h is Planck's constant, ν is the photon's frequency, α is the absorption coefficient, and A is a proportionality constant [16]

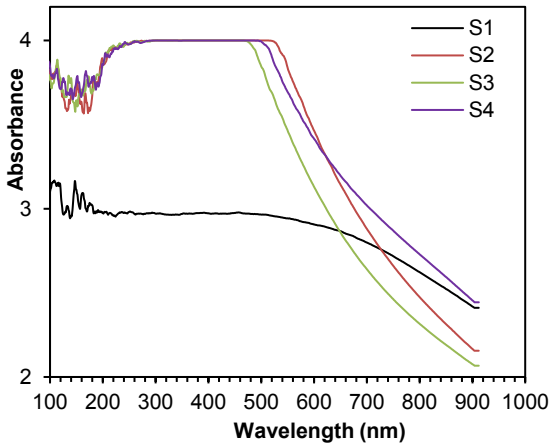

Fig. (4) UV–visible absorption spectra of Cs/PANI blends (S-series) with varying LiI salt concentrations

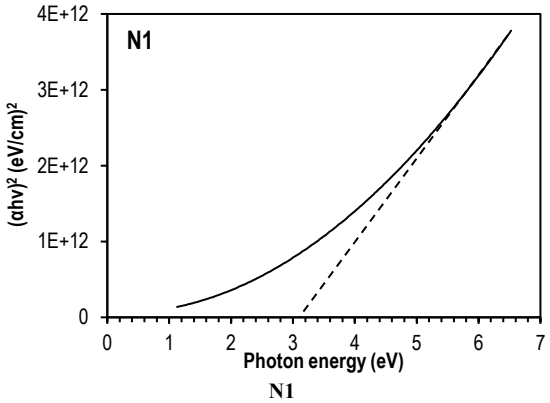

N1

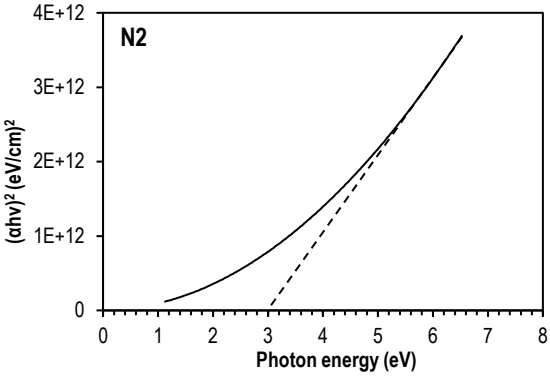

N2

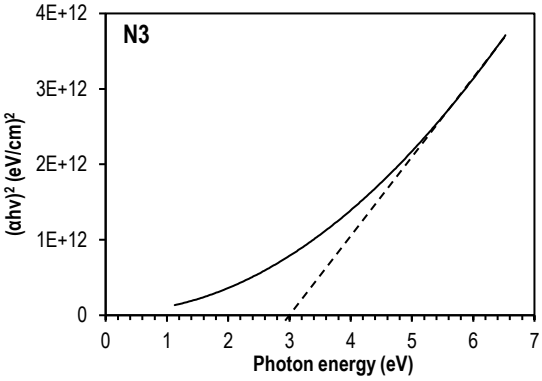

N3

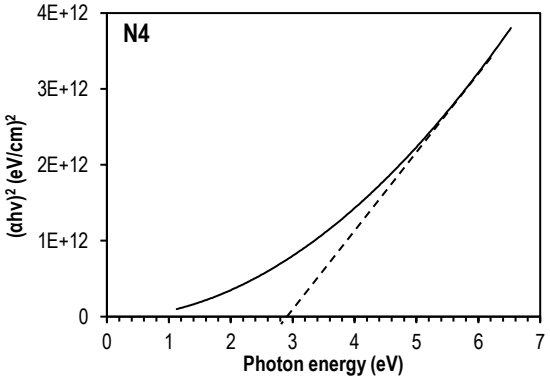

N4

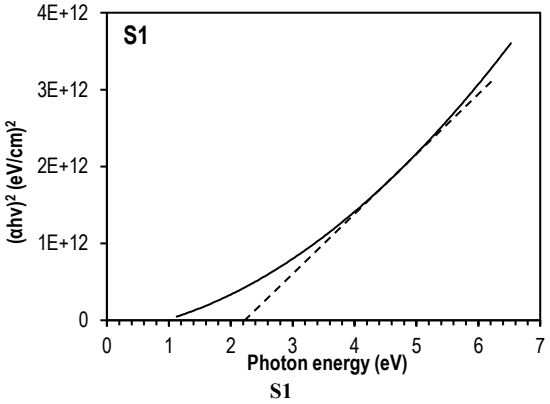

S1

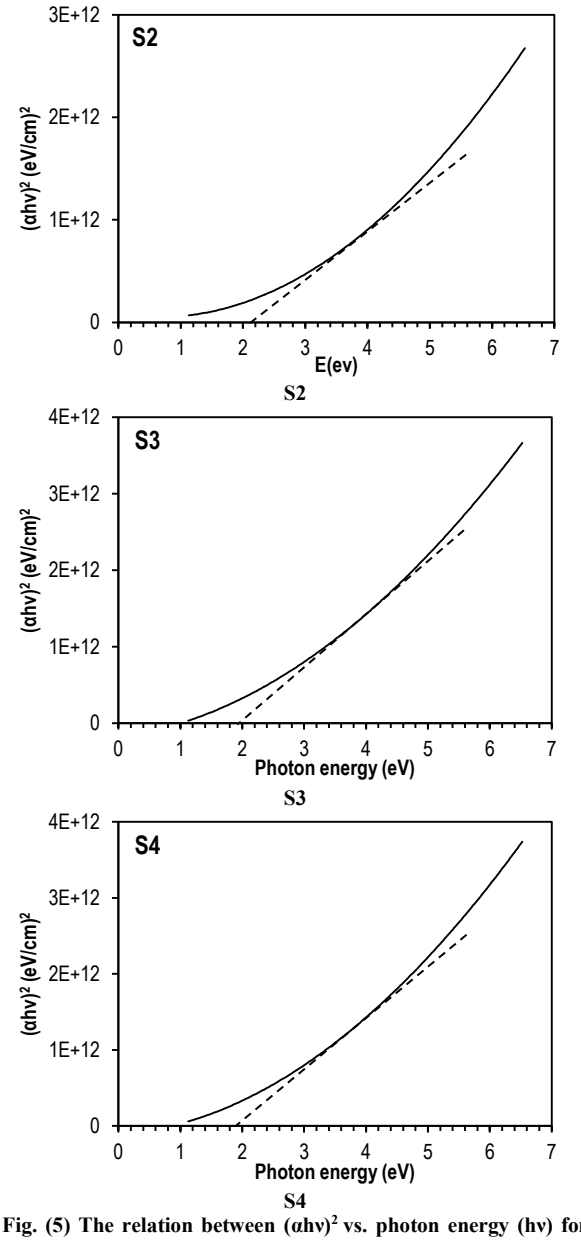

Fig. (5) The relation between $(\alpha hv)^2$ vs. photon energy (hv) for groups (a) N and (b) S

Table (6) Optical band gap of groups N and S

Assignment	E_g (eV)	Group
N1	3.1	Group N (NaI)
N2	3.0	
N3	2.9	
N4	2.8	
S1	2.2	Group S (LiI)
S2	2.1	
S3	2.0	
S4	1.9	

Figure (6) illustrates the relationship between dielectric loss (log σ) and the inverse temperature (1000/T, K^{-1}) for the NaI-doped Cs/PANI samples (N1–N4). Measurements were conducted across a defined temperature range to investigate the ionic and electronic transport behavior as well as the dielectric relaxation characteristics of the samples. All samples exhibit a clear temperature-dependent dielectric response, with log σ increasing as temperature rises (i.e., at lower 1000/T values). A broad relaxation region is observed in each curve, whose intensity and position vary with salt concentration. The samples with an increased concentration of NaI (N3 and N4) have very high values of dielectric losses and relaxation peaks that shift to high temperatures as opposed to the low salt samples (N1 and N2). In addition, the gradient of the high-temperature region increases steeper at higher salt content indicating the increasing thermal activation and charge transportation. These tendencies could be attributed to two major processes:

(1) Higher concentration of mobile charge carriers- Adding of NaI takes the form of more Na^+ and I^- ions and they increase the concentration of the free charge carriers. As a result, dielectric loss (σ) grows since more charges are available to react to the fluctuating electric field that increases the conductive part of the dielectric answer.

(2) Alteration of polymer chain dynamics and ion polymer interactions- The salt added can be used as a plasticizer, enhancing the polymer chain mobility and promoting ion hopping. This enhances chain movements reducing the energy barrier to charge transfer and hence increasing ionic conductivity. At very high salt concentrations, however the ion pairing or clustering can take place that narrows or shifts a relaxation peak to some degree and restricts further gains of conductivity. Overall, as the NaI concentration increases, both the dielectric loss and conductivity responses rise across the entire temperature range. The shift of the relaxation peak toward higher temperatures and the increase in its amplitude confirm that higher NaI content enhances ionic mobility and thermal activation within the Cs/PANI matrix [17]. The ionic conductivity (σ) was calculated using the following equation:

$$\sigma = \frac{L}{Rb * A} \qquad (2)$$

where L =1.5 cm thickness of film, Rb the impedance of sample and A = 1.77 cm^2 the mean area of the electrodes [18]

Figures (7a,b) collectively illustrate the temperature and composition dependent ionic conductivity behavior of the Cs/PANI/LiI electrolytes. Figure (7a), the plot of *log σ* versus 1000/T (K^{-1}) exhibits a non-linear dependence characteristic of Vogel–Tammann–Fulcher (VTF) behavior, suggesting that ionic conduction in these polymer electrolytes is governed primarily by segmental motion of the polymer chains, rather than by simple thermally activated ion hopping. The increase in conductivity with temperature up to an optimal point—followed by a slight decline—indicates that enhanced segmental mobility initially facilitates ion transport. Nevertheless, when the temperature is elevated, thermal agitation can cause multi-distribution

of ions and loss of structural strength to the Polymer network. The chronological increase of the curves (S1-S4) also proves the fact that the concentration of LiI is gradually increasing and the ionic conductivity is increasing, which indicates the increase of the concentration of the mobile Li^+ ions and the availability of the charge carriers in the polymer structure.

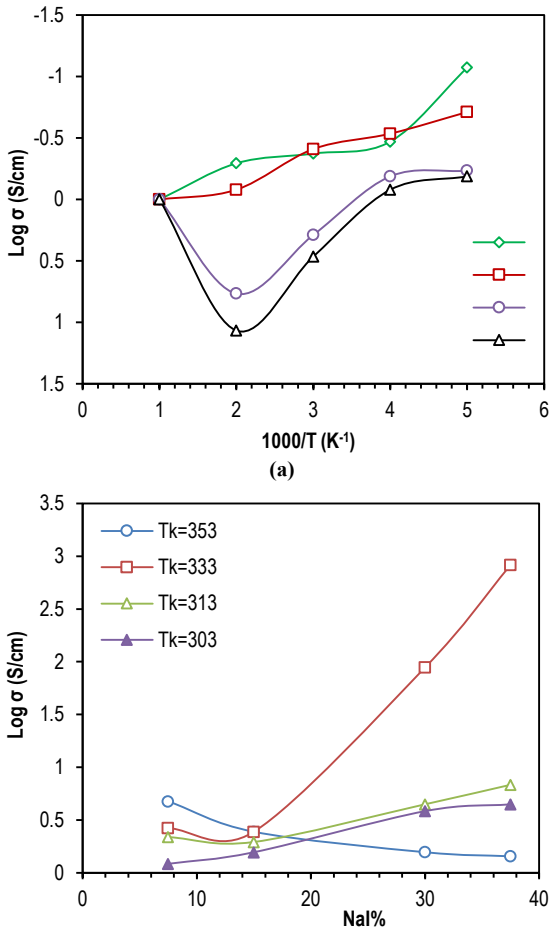

Fig. (6) Ionic conductivity of Cs/PANI blends (NaI series): (a) temperature dependence of conductivity and (b) ionic conductivity as a function of NaI concentration

The same trend is supported by Fig. (7b) which is a variation of the ionic conductivity (σ) as a function of LiI weight percentage at various temperatures (303-353 K). Both temperature and LiI concentration have a very strong positive relationship with conductivity, which validates that LiI is a good dopant that promotes ionic movement by generating charge carriers as well as due to the plasticizing influence of Li-polymer interactions. The rapid rise in conductivity with increasing LiI concentration especially at high temperature is in tandem with the increasing values of *log* σ as shown in Fig. (7a), which is a testament to the strong interactive role of temperature and salt mixture on ionic transport. In general, the findings are indicative of the fact that ionic conductivity in the Cs-PANI-Li polymer electrolyte system is highly sensitive to temperature and LiI content with the two factors having the combined effect on decreasing the segmental dynamics and charge transport mechanisms within the polymer matrix [19,20].

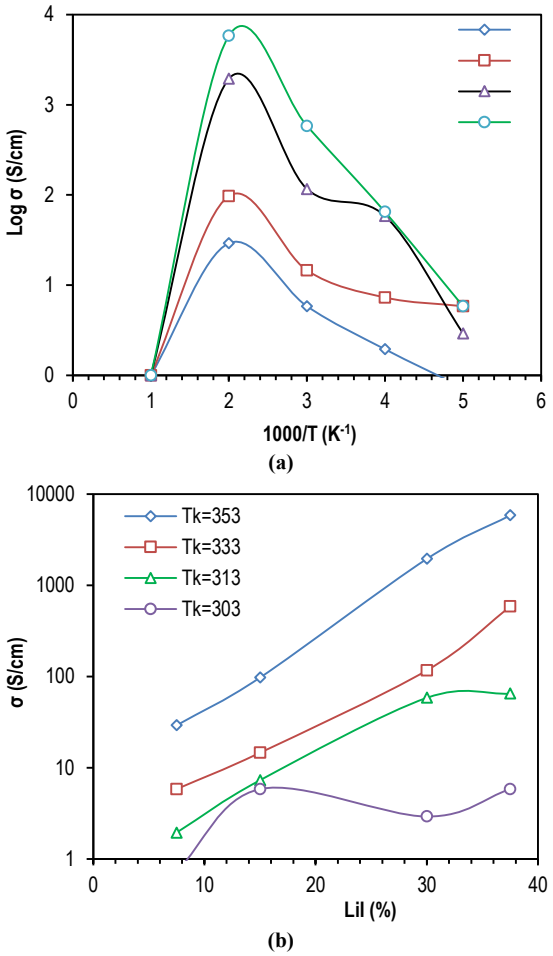

Fig. (7) Blend electrolytes S: (a) conductivity temperature dependence; (b) change of conductivity with the percent weight percentage of LiI

Figure (8) shows how the real dielectric constant (ε_r) and variation of frequency varies with the proportions of sodium iodide (NaI). The real parts of dielectric constant (ε_r) values were obtained using the following equation [21]:

$$\varepsilon_r = \frac{Z_i}{\omega\, C_0 (Z_r^2 + Z_i^2)} \qquad (3)$$

where ω is the angular frequency (ω=2πf), C_0 is vacuum capacitance and Zr and Zi are real and imaginary parts of resistance [22]

The curves indicate that the behaviors of all the samples is typical, i.e. the dielectric constant rises with low frequencies and then rises gradually and substantially as the frequency goes on. This is characteristic of polymer materials and electrolytic membranes that are based on the ion transport. At low frequencies, dipoles and free ions can follow the quick oscillations of the electric field successfully and result

in the overall better polarization of the material and, therefore, an increase in the dielectric constant. At higher frequencies, the available time to reposition oneself in time becomes limited and insufficient, and it is no longer possible to maintain alignment of the dipoles and free ions with the external electric field. This causes a slow reduction in the strength of polarization and consequently, the dielectric constant reduces. Such a behavior is in line with numerous polarization processes including ionic polarization. All the dipole and borderline constants decrease with high frequencies. Conversely, the findings depict that the relative ranking of the samples with regards to the value of dielectric constant involves a definite pattern which is, again, dependent on salt concentration and thus the samples could be ranked in relative order as follows: N4>N3>N2>N1. The sample N4 exemplifies the maximum value of the dielectric constant because its salt concentration is higher and more ions are released in the polymer network and ionic and polaron polarization, therefore, increasing the value of dielectric constant considerably. Sample N1 that has the minimum amount of salt has the minimum value of the dielectric constant. It means that the amount of mobile charges dropped by some percentage, and the contribution to polarization processes has been decreased. This action is completely in agreement with all other electrical findings of these samples since the samples with better conductivity (and more so N4) possess better dielectric constants which lead to the conclusion that the higher the salt concentration the better the electrical conductivity as well as dielectric properties of such samples are [23].

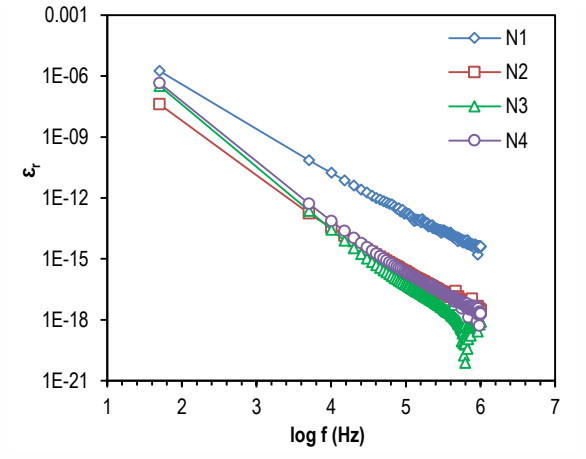

Fig. (8) Real dielectric constant (ε_r) vs. frequency of group N (salt NaI)

Figure (9) depicted the variation of dielectric constant for the samples S1–S4, which exhibited a clear difference in dielectric behavior with changing frequency. The results indicated that sample S1 possessed the highest relative permittivity value at low frequencies. This is attributed to the effectiveness of dipole polarization mechanisms and phase boundary polarization resulting from the presence of freer ions and their ability to track the slowly changing electric field. As the salt content increased in samples S2, S3, and S4, a gradual and continuous decrease in the dielectric constant values was observed across the frequency range. This behavior is explained by the formation of ion pairs and salt clusters that reduce the free ion mobility within the polymer matrix. The semiconducting nature of polyaniline also contributes to this effect. As the salt concentration increases, partial conduction pathways form within the material, reducing the effectiveness of polarization and leading to a decrease in the measured permittivity. Thus, the transition from S1 to S4 reflects a shift from a strongly polarized system to one with predominantly conductive behavior, and a transformation of the ions into less electrically responsive clusters [24].

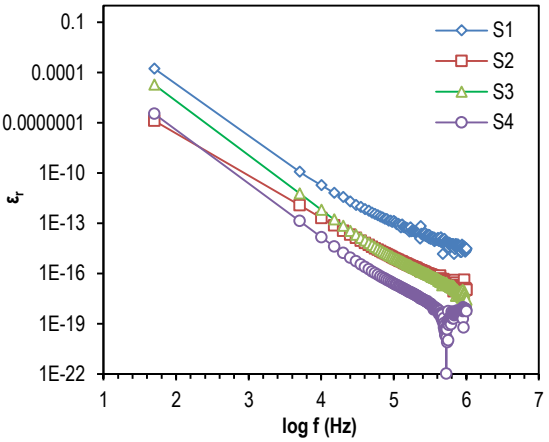

Fig. (9) Real dielectric constant (ε_r) vs. frequency of group S (salt LiI)

4. Conclusion

In this study, chitosan–polyaniline blend electrolytes with NaI and LiI salts were successfully prepared using the solution casting method. FTIR analysis confirmed the interaction between the polymer matrix and the incorporated salts through coordination with oxygen- and nitrogen-containing functional groups. UV-visible spectroscopy showed enhanced optical absorption and a gradual reduction in the optical band gap with increasing salt concentration, indicating improved electronic transitions within the polymer matrix. Electrical conductivity measurements revealed that conductivity increases with temperature and salt concentration. The samples with LiI exhibiting higher conductivity than NaI-based samples due to the higher mobility of Li^+ ions. Dielectric analysis demonstrated typical frequency-dependent behavior associated with polarization mechanisms and ion transport in polymer electrolytes.

Acknowledgment

The researchers would wish to acknowledge the support of The Department of Physics, College of Science at the University of Baghdad for this research.

References

[1] F.M. Ahmed and M.K. Jawad, "Nanocomposites electrolytes based conductive polymer for electrochemical application", *J. Theor. Appl. Phys.*, Special Issue (AICIS'23) (2024) Article 23.

[2] A.M. Qusay and M.K. Jawad "Investigation of Optical and Electrical properties of Solid Polymer Electrolyte based on Natural polymer", *Iraqi J. Phys.*, 23(3) (2025) 75-78.

[3] G.E.A. Awad et al., "Functionalized κ-carrageenan/hyperbranched poly(amidoamine)for protease immobilization: Thermodynamics and stability studies", *Int. J. Biol. Macromol.*, 148 (2020) 1140-1155.

[4] D. Zhang et al., "Solid polymer electrolytes: Ion conduction mechanisms and enhancement strategies", *Nano Res. Ener.*, 2(2) (2023) e9120050.

[5] D. Zhang et al., "Solid polymer electrolytes: Ion conduction mechanisms and enhancement strategies", *Nano Res. Ener.*, 2(1) (2023) 9120050.

[6] Y.L. Yap, A.H. You and L.L. Teo, "Preparation and characterization studies of PMMA–PEO-blend solid polymer electrolytes with SiO_2 filler and plasticizer for lithium ion battery", *Ionics*, 25(3) (2019) 1307–1318.

[7] S.K. Shetty et al., "Sodium iodide dopant mediated enhancements in energy storage characteristics of polysaccharide polymer electrolytes", *J. Ener. Stor.*, 95 (2024) Article 112553.

[8] K. Suvarna et al., "Investigation of solid bio-membrane based on corn biomass as a proton-conducting bio-electrolyte", *Bull. Mater. Sci.*, 46 (2023) Article 112.

[9] M. Teodorescu, M. Bercea and S. Morariu, "Biomaterials of PVA and PVP in medical and pharmaceutical applications: perspectives and challenges", *Biotechnol. Adv.*, 36(1) (2018) 44-60.

[10] A. Abed et al., "Polyester-supported Chitosan–Poly(vinylidene fluoride) composite membranes: structural and electrical properties", *Chinese J. Polym. Sci.*, 37(3) (2019) 321-330.

[11] M. Andonegi et al., "Structure–property relationships of chitosan/collagen films with potential biomedical applications", *Carbohydr. Polym.*, 237 (2020) Article 116159.

[12] C. Rodrigues et al., "Mechanical, Thermal, and Barrier Properties of Chitosan-Based Nanocomposite Films for Food Packaging", *J. Polym. Environ.*, 28 (2020) 1216-1236.

[13] J. Kumirska et al., "Application of Spectroscopic Methods for Structural Analysis of Chitin, Chitosan and Their Derivatives", *Mar. Drugs*, 8(6) (2010) 1568-1615.

[14] B.R. Pasela et al., "Synthesis and Characterization of Acetic Acid-Doped Polyaniline and Polyaniline–Chitosan Composite", *Biomimetics*, 4(1) (2019) 15-23.

[15] H.A. Mohammed, P.A. Mohammed and S.B. Aziz, "Investigation of optical band gap in PEO-based polymer composites doped with green-synthesized metal complexes using various models", *RSC Adv.*, 15 (2025) 23319-23341.

[16] L. Colombo, **"Solid State Physics, A Primer"**, Ch. 8, IOP Pub. (Bristol, 2021), pp. 1-31.

[17] A. Arya and A.L. Sharma, "Effect of Salt Concentration on Dielectric Properties of Li-Ion Conducting Blend Polymer Electrolytes", *J. Mater. Sci.: Mater. Electron.*, 29(20) (2018) 17903-17920.

[18] H. Ohno, **"Electrochemical Aspects of Ionic Liquids"**, Wiley & Sons, Inc. (2005).

[19] K.M. Diederichsen, H.G. Buss and B.D. McCloskey, "The Compensation Effect in the Vogel–Tammann–Fulcher (VTF) Equation for Polymer-Based Electrolytes", *Macromolecules,* 50(10) (2017) 3831-3840.

[20] Y. Zhao et al., "Ionic Conduction in Polymer-Based Solid Electrolytes", *Adv. Sci.*, 10 (2023) 2201718.

[21] E.A. Swady and M.K. Jawad, "Dependency of the AC conductivity of blend nanocomposites on the Lil and ZnO percent", *AIP Conf. Proc.*, 2437(1) (2022) 020053.

[22] F.M. Ahmed and M.K. Jawad, "Characterization of Blend Electrolytes Containing Organic and Inorganic Nanoparticles", *Iraqi J. Appl. Phys.*, 20(1) (2024) 43-50.

[23] E.A. Swady and M.K. Jawad, "Study FTIR and AC Conductivity of Nanocomposite Electrolytes", *Iraqi J. Phys.*, 19(51) (2021) 15-22.

[24] A.M.A. Mohamed, M.I.N. Isa and H.Z. Abidin, "The effect of lithium iodide on the structural and dielectric properties of chitosan-based polymer electrolytes", *J. Non-Cryst. Solids*, 463(1) (2017) 61-71.

